Functional differences between neurotransmitter binding sites of muscle acetylcholine receptors

Tapan K. Nayak[a], Iva Bruhova[a,1], Srirupa Chakraborty[a,b,1], Shaweta Gupta[a], Wenjun Zheng[b], and Anthony Auerbach[a,2]

[a]Department of Physiology and Biophysics, State University of New York at Buffalo, Buffalo, NY 14214; and [b]Department of Physics, State University of New York at Buffalo, Buffalo, NY 14260

Edited by Jean-Pierre Changeux, CNRS, Institut Pasteur, Paris, France, and approved November 5, 2014 (received for review July 28, 2014)

A muscle acetylcholine receptor (AChR) has two neurotransmitter binding sites located in the extracellular domain, at αδ and either αε (adult) or αγ (fetal) subunit interfaces. We used single-channel electrophysiology to measure the effects of mutations of five conserved aromatic residues at each site with regard to their contribution to the difference in free energy of agonist binding to active versus resting receptors (ΔG_{B1}). The two binding sites behave independently in both adult and fetal AChRs. For four different agonists, including ACh and choline, ΔG_{B1} is ∼−2 kcal/mol more favorable at αγ compared with at αε and αδ. Only three of the aromatics contribute significantly to ΔG_{B1} at the adult sites (αY190, αY198, and αW149), but all five do so at αγ (as well as αY93 and γW55). γW55 makes a particularly large contribution only at αγ that is coupled energetically to those contributions of some of the α-subunit aromatics. The hydroxyl and benzene groups of loop C residues αY190 and αY198 behave similarly with regard to ΔG_{B1} at all three kinds of site. ACh binding energies estimated from molecular dynamics simulations are consistent with experimental values from electrophysiology and suggest that the αγ site is more compact, better organized, and less dynamic than αε and αδ. We speculate that the different sensitivities of the fetal αγ site versus the adult αε and αδ sites to choline and ACh are important for the proper maturation and function of the neuromuscular synapse.

allosteric protein | ion channel | ligand binding sites | single-channel electrophysiology | synaptic maturation

Receptors at synapses respond to specific chemical signals in the extracellular environment because the active conformation of the protein has a higher affinity for the ligand compared with the resting conformation (1, 2). The active vs. resting difference in binding free energy increases the relative stability of the active state and, hence, the probability of a cellular response. In this report, we describe and distinguish sources of ligand-binding free energy in three kinds of agonist site present in mouse muscle nicotinic acetylcholine receptors (AChRs). Our goal was to use single-channel electrophysiology to assess the relative contribution of significant functional groups to the overall free energy generated by the affinity change at each type of site.

At cholinergic synapses, the main chemical signals are ACh released from nerve terminals and choline, which is an ACh precursor, hydrolysis product, and stable component of serum (3). The muscle AChR has central pore surrounded by five subunits of composition $\alpha_2\beta\delta\varepsilon$ in adult-type and $\alpha_2\beta\delta\gamma$ in fetal-type (Fig. 1*A*) (4). The fetal, γ, subunit is essential for proper synapse maturation, and the adult, ε, subunit is necessary for proper function of mature synapses (5–7). Each AChR pentamer has two agonist binding sites in the extracellular domain, at αδ and either αε (adult) or αγ (fetal) subunit interfaces.

The change in agonist affinity occurs within the global, resting↔active "gating" conformational change. Structural rearrangements at agonist sites that generate the affinity change are akin to movements of S4 in voltage-gated channels that generate gating currents. Given the central role of receptors at synapses, we thought it important to understand in detail the components of the free energy change that undergird the agonist affinity change. In wild-type AChRs, a large, uphill gating energy without agonists ensures the system will rarely activate constitutively, and a large, downhill free energy generated by affinity increases at the two agonist sites ensures that the protein will be active with a high probability after the release of ACh from the motor nerve terminal (8).

We have estimated the free energy contributions of eight functional groups of five conserved residues at three different kinds of muscle AChR agonist site (αδ, αε, and αγ). On the α side of each site, there are four aromatics known to influence agonist affinity: αY190 (in loop C), αY198 (loop C), αY93 (loop A), and αW149 (loop B) (Fig. 1) (9–13). In addition, there is a conserved tryptophan in the nonα subunit, W55 (at position 57 in the δ subunit) (11, 14–16). In fetal AChRs, αW149 and αY198 have been shown to stabilize the quaternary ammonium of the agonist by cation-π forces (10, 13, 17).

Previously, estimates of the ACh-binding free energy difference in mouse adult-type receptors after mutations indicated that only three of the mentioned aromatics (αY190, αY198, and αW149) are important (18), and other experiments showed that the free energy difference from both agonist sites combined is greater in fetal vs. adult AChRs (19). Here, we extend and refine these estimates. First, we measured the change in the net binding free energy after a mutation of each aromatic side chain in AChRs having just one functional binding site, so that the αδ, αε, and αγ sites could be probed independently, rather than pairwise. Second, we made some of these measurements using three partial agonists in addition to ACh, including the physiological ligand choline. Third, we estimated the degree of free energy coupling between some of the aromatic side chains at the fetal, αγ, site. Fourth, we used molecular dynamics (MD) simulations to estimate ACh binding energies and suggest structural correlates for differences between the three types of agonist site. We hypothesize that

Significance

We present here energy measurements for agonist binding to adult and fetal neuromuscular junction acetylcholine receptors. We identify the chemical groups at the three functionally different types of transmitter binding site (αγ, αδ, and αε) that generate energy from the agonist for channel gating. We also predict the structural correlates of the energy differences from experiments and molecular dynamics simulations. This article is of general interest because it is the first time to our knowledge that single ligand-binding-site energies have been measured in any receptor. In addition, the results provide a rationale for understanding the required receptor subunit swap in synapse maturation (a long-standing and unsolved problem), as well as the structural basis for agonist efficacy.

Author contributions: T.K.N. and A.A. designed research; T.K.N., I.B., S.C., and S.G. performed research; T.K.N. contributed new reagents/analytic tools; T.K.N., I.B., S.C., S.G., and W.Z. analyzed data; and T.K.N. and A.A. wrote the paper.

The authors declare no conflict of interest.

This article is a PNAS Direct Submission.

[1]I.B. and S.C. contributed equally to this work.

[2]To whom correspondence should be addressed. Email: auerbach@buffalo.edu.

This article contains supporting information online at www.pnas.org/lookup/suppl/doi:10.1073/pnas.1414378111/-/DCSupplemental.

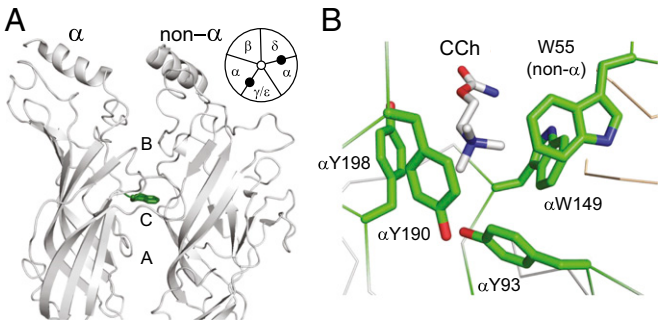

Fig. 1. Ligand binding sites. (*A*) Side view of a muscle AChR [*Torpedo marmorata*; PDB ID code 2bg9 (34)] showing an agonist site in the extracellular domain (αW149 and loops A, B, and C are marked). (*Inset*) Each AChR has two sites (filled circles) at αδ and αε (adult) or αγ (fetal) subunit interfaces. (*B*) High-resolution view of the ligand binding site of an acetylcholine binding protein occupied by carbamylcholine (CCh) [*Lymnaea stagnalis;* PDB ID code 1uv6 (11)]. Aromatic residues are labeled using mouse AChR numbering.

a greater sensitivity of fetal vs. adult AChRs to choline is a reason for the γ→ε subunit swap required for proper maturation of the neuromuscular synapse.

Results

Agonists. The free energy generated at each site by the affinity change for the agonist is the difference between high-affinity (HA; to the active conformation) and low-affinity (LA; to the resting conformation) binding free energies:

$$\Delta G_{B1} = G_{HA} - G_{LA} \quad [1]$$

This energy is proportional to the log of the ratio of gating equilibrium constants, with one vs. without any agonists (*SI Appendix*, Fig. S1). In wild-type (WT) AChRs that have two agonist binding sites, the total free energy from both affinity changes was estimated from single-channel current interval durations obtained at a saturating agonist concentration, using constructs having known unliganded gating equilibrium constants (Fig. 2*A* and *SI Appendix*, Fig. S2). Fig. 2*B* (*SI Appendix*, Table S1) shows this total energy from two-site AChRs for four different agonists. Fetal-type AChRs, which have a γ-subunit rather than an ε-subunit, provide >1.5 kcal/mol more favorable free energy for all agonists compared with adult-type. Without this extra free energy from fetal AChRs, the diliganded gating equilibrium constant would be ∼30-fold lower and the synaptic current peak ∼1/3 smaller.

To identify how the total agonist-binding free energy difference is divided between the two agonist sites, we measured the gating equilibrium constants using AChRs that had only one functional site and calculated the net free energy from each. In these constructs, one binding site was WT and the other was knocked out by a mutation or mutations in the complementary, nonα subunit (20). We added distant background mutations and depolarization to facilitate the measurements, but these only changed the unliganded gating equilibrium constant and had no effect on the free energy of the affinity change (21). In what follows, all values have been corrected for the effect of the background and pertain to WT AChRs at a membrane potential of −100 mV.

The results for four agonists and three different one-site AChRs are shown in Fig. 2*C* (*SI Appendix*, Table S2). The two adult sites (αδ and αε) each supply approximately equal free energies from ACh, but the fetal, αγ, site provides ∼−2.1 kcal/mol more favorable energy from the neurotransmitter. We repeated these experiments using choline (Cho), carbamylcholine (CCh), or tetramethylammonium as the agonist (*SI Appendix*, Fig. S3). As with ACh, the αγ site provides ∼−2 kcal/mol more favorable energy from these ligands. Cho is a weak, partial agonist at αε and αδ but a strong one at αγ, where it provides only slightly less energy for gating than ACh at the adult sites. As a consequence, fetal AChRs generate a larger response to Cho compared with adult AChRs. ΔG_{B1} at αε vs. αδ was about the same for ACh, CCh, and tetramethylammonium but was less favorable for Cho at αε. The relative ACh and Cho free energies at each site are summarized in Fig. 2*E*.

For all agonists, the sum of the one-site energies (αδ+αε or αδ+αγ) was approximately equal to the total binding energy difference measured in AChRs having two functional sites (Fig. 2*D*). This indicates that the binding sites behave approximately independently, insofar as free energy from the agonist is concerned.

Tryptophans. A candidate for providing the extra free energy from the αγ site was γW55, in the nonα subunit (Fig. 1*B*). We measured the change in ΔG_{B1} from altering just this side chain at each site by substituting an A in the δ, ε, or γ subunit (Fig. 3). These experiments were carried out using either two-site AChRs (with the companion site WT) or one-site AChRs (with the companion site knocked-out by mutation; Fig. 3*A*) (*SI Appendix*, Table S3). The effects were approximately the same in both conditions, which indicates that the A substitution did not disrupt the essential independence of the two sites.

The W55A substitution reduced the favorable ΔG_{B1}^{ACh} energy at αγ and αε but had almost no effect at αδ (Fig. 3*B*). The largest effect by far was at αγ, where the change was $\Delta\Delta G_{B1}^{ACh}$∼+4.5 kcal/mol, which is ∼60% of the total free energy from this site. The effect of the W55A substitution was more modest at αε (∼+1.2 kcal/mol; ∼25%) and was nil at αδ. For the δW57A+γW55A

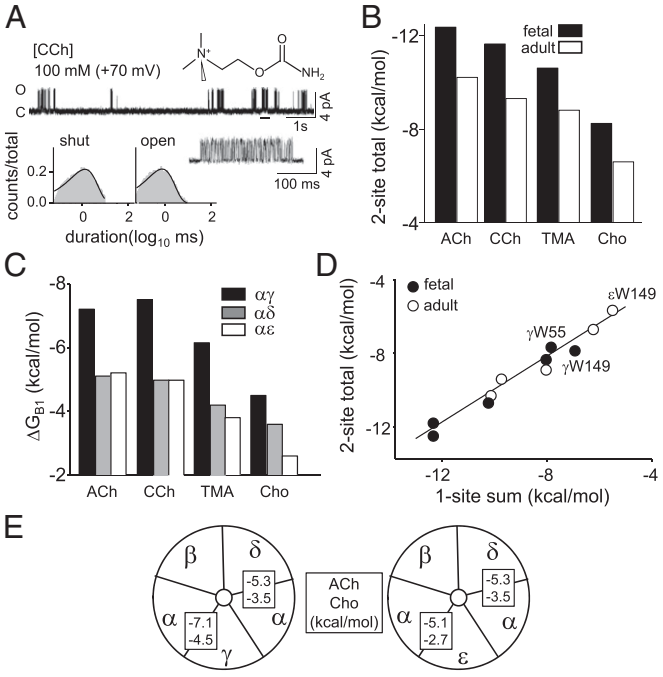

Fig. 2. Free energies from the affinity change. (*A*) Example single-channel currents and interval-duration histograms (fetal AChRs, 100 mM CCh; V_m = +70 mV; open is up). (*Top*) Low-resolution trace showing clusters of gating activity from individual AChRs; silent, intercluster intervals are desensitization (underlined cluster shown at higher resolution below). (*Bottom*) Cluster interval duration histograms fitted by a single exponential (solid line). After correcting for the background (βT456I + δI43H), $G_2^{CCh,WT}$ = −1.7 and (ΔG_{B1}+ΔG_{B2})^{CCh,WT} = −11.6 kcal/mol (*SI Appendix*, Fig. S1). (*B*) Different agonists. For all ligands, the total free energy from both sites combined is >−1.5 kcal/mol more favorable in fetal AChRs. (*C*) AChRs having only one functional agonist site. For all agonists, ΔG_{B1} at αγ is the most favorable. (*D*) The free energy from site pairs is approximately equal to the sum of single sites (linear slope = 0.90 ± 0.03; r^2 = 0.95). (*E*) ΔG_{B1}^{ACh} and ΔG_{B1}^{Cho} at each site.

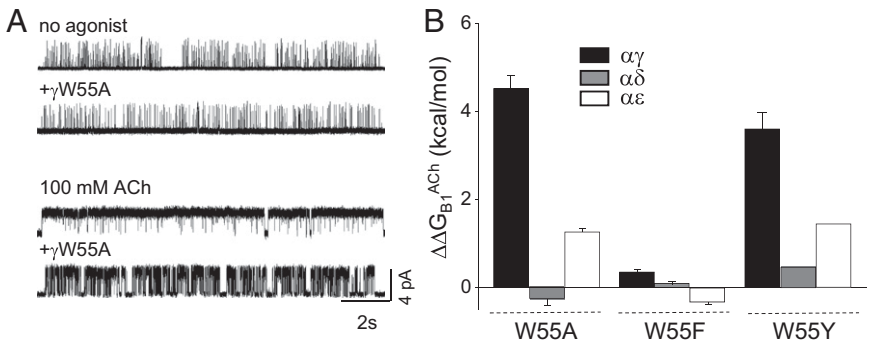

Fig. 3. W55 mutations at single agonist sites. (*A*) The γW55A mutation hardly affects unliganded gating (*Top*) but substantially reduces the liganded gating (*Bottom*), because of a loss in favorable ΔG_{B1}^{ACh} (βL262S + δL265S + δP123R background; V_m = +70 mV; open is up). (*B*) The change in ΔG_{B1}^{ACh} consequent to W55A and F mutations at αγ, αδ, and αε sites (positive is a loss of favorable free energy, which was greatest at αγ; *SI Appendix*, Table S3).

combination, the total loss in ACh free energy was about the same as the sum from the one-site experiments (Fig. 2*D*), which is again consistent with site independence. We also measured the effect of the γW55A substitution, using Cho as the agonist. As with ACh, this mutation reduced the free energy from affinity change at the αγ site by a large amount (~55% of the total) (Fig. 3). The greater efficacy of Cho in fetal-type AChRs can be attributed mainly to the action of γW55.

In a final set of experiments with W55, we replaced the indole with either a benzene ring or a tyrosine side chain (F or Y substitution) (Fig. 3 and *SI Appendix*, Table S3). F substitutions had little or no effect on ΔG_{B1}^{ACh} at any of the three binding sites (<0.5 kcal/mol), whereas Y substitutions showed a similar trend as for alanine, with energy losses at αγ>αε>αδ.

We next investigated the free energy provided by the agonist affinity change after an A substitution at the other binding site tryptophan, αW149. In two-site AChRs, this mutation (in both α subunits) makes the total ACh energy less favorable by ~+4.6 kcal/mol in both adult and fetal AChRs (*SI Appendix*, Table S3).

Fig. 4*A* shows that the single-site breakdown of the αW149A free-energy changes. We did not examine the αδ and αε sites separately, but estimated ΔG_{B1}^{ACh} values for these single sites by dividing the total energy change in two-site adult pentamers in half (assuming equal free energy changes at each site). The losses in favorable energy from the three sites were similar, but not identical, with that at αγ being somewhat larger than that at αδ/αε. From the αW149A point mutations, we estimate that for ACh at the αγ site, the deletion of the αW149 indole results in a loss of $\Delta\Delta G_{B1}^{ACh}$ ~+3.0 kcal/mol, which is modestly greater than the average of ~+2.3 kcal/mol at αδ/αε (*SI Appendix*, Table S3). However, at αγ, the mutation αW149A has a substantially smaller effect than γW55A, whereas at αε and αδ, the order is reversed.

Tyrosines. The α-subunit side of the agonist binding pocket has three conserved tyrosines: αY198 and αY190 in loop C and αY93 in loop A (Fig. 1*B*). We measured the change in ΔG_{B1}^{ACh} in one-site AChRs having a F substitution at each of these, which removes the –OH but leaves the benzene ring intact (Fig. 4*A* and *SI Appendix*, Table S4). αY198F had a negligible effect at all three binding sites. αY93F also had a small consequence at αε and αδ but incurred a slightly greater penalty at αγ. αY190F, however, made ΔG_{B1}^{ACh} substantially less favorable at all three binding sites, by ~+1.9 kcal/mol.

We next measured ΔG_{B1}^{ACh} in receptors having a single, functional αγ site with an A substitution at each of the three α-subunit tyrosines (both α subunits mutated) (Fig. 4*B*). As with αW149, we estimated the corresponding values for αδ and αε single sites by dividing the total energy change in two-site adult AChRs in half. The changes in ΔG_{B1}^{ACh} for αF190A, αF198A, and αF93A at αδ/αε were +1.9, +1.9, and +0.7 kcal/mol, respectively (*SI Appendix*, Table S4). The corresponding values at αγ were +1.8, +2.4, and +2.0 kcal/mol. These are the $\Delta\Delta G_{B1}^{ACh}$ free energy losses consequent to the deletion of each benzene ring. This loss was substantially greater at αγ vs. αδ/αε only for αY93.

To summarize (Fig. 4*E*), the aromatic groups of the two loop C tyrosines and αW149 provide similar free energies at all three binding sites (~−2 kcal/mol). However, the aromatic group of αY93 and, in particular, W55 has more favorable effects at αγ. Only three of the aromatics contribute to ΔG_{B1}^{ACh} at the αε and αδ sites, whereas all five contribute at the fetal, αγ, site. Regarding the tyrosine hydroxyl groups, only that of αY190 makes a large contribution (~−2 kcal/mol) that is similar at all three sites.

Coupling. The five binding site aromatic amino acids are in close proximity, and we sought to learn how these side chains share ΔG_{B1}^{ACh} at the αγ site. Such free energy coupling must take place because the sum of the energy losses after alanine point mutations exceeds the total $\Delta\Delta G_{B1}^{ACh}$. At all three sites, the sum of the free energy losses for A substitutions of the five aromatic residues is about twice the apparent $\Delta\Delta G_{B1}^{ACh}$. Notice that a change in ΔG_{B1}^{ACh} after an A substitution is a function of both the loss from the removal of side chain itself and the ability of other structural elements to fill the gap [the A substitution itself has little effect (18)].

The results so far indicate that the αγ site differs from the two adult-type agonist sites insofar as deletion of the aromatic groups from W55 and, to a lesser extent, αY93 and αW149 result in a greater loss of favorable binding free energy. To further probe the character of αγ, we measured coupling between side chains by making pairwise A substitutions in one-site constructs (other site knocked out). The only functional site was αγ, which had a γW55A mutation plus an A at αW149, αY190, αY198, or αY93. We only probed pairwise interactions with γW55 and not between the α subunit aromatics.

The coupling free energies, which are the differences between the net and the sum ΔG_{B1}^{ACh} values, are shown in Fig. 4*C* (*SI Appendix*, Fig. S4 and Table S5). γW55A interacts significantly with αY93A and αY190A and modestly with αW149A, but not at all with αY198A. For the three interacting residues, the free energy loss in the A–A pair was in all cases less than the sum of the single A substitutions. Apparently, at the αγ site, αY93 and αY190 can each replace ~50% of the lost favorable energy caused by the deletion of the γW55 indole.

The αY190 –OH group makes a substantial contribution to ΔG_{B1}^{ACh} at all three sites (~−1.7 kcal/mol; *SI Appendix*, Table S4). We measured coupling between αY190F and γW55A and found it to be small (Fig. 4*C*).

Simulations. To explore possible mechanistic bases for the experimental free energy measurements, we carried out MD simulations using simple homology models of each of the three kinds of agonist site. There are two issues to consider in making comparisons between simulated and experimental energy estimates. First, the simulations estimate a bound vs. unbound energy difference, whereas the ΔG_{B1} measurements from electrophysiology give a difference in binding free energy: HA minus LA (Eq. **1**). In adult-type AChRs, for the agonists and mutations used in this study, the HA and LA equilibrium dissociation constants are correlated and have the relationship $G_{HA} \sim 2G_{LA}$ (22). Combining this with Eq. **1**,

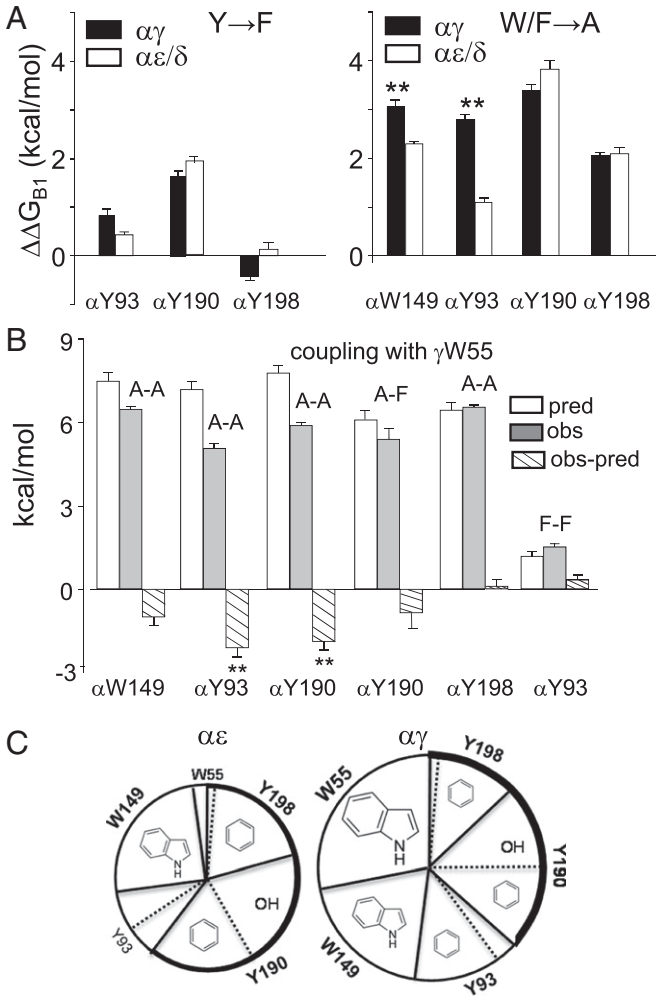

Fig. 4. Effects of mutations of aromatic residues at single-agonist sites. (*A*, *Left*) Removal of the tyrosine hydroxyl had the largest effect on ΔG_{B1}^{ACh} at αY190 and was similar at αγ vs. αε/δ. (*Right*) Removal of the aromatic group was similar at αY190, αW149, and αY93 at αγ. The effect was greater at αγ vs. αδ/αε only at αW149 and αY93 (mean ± SEM; $n \geq 3$ patches). **Significance at 95% confidence interval. (*B*) Coupling between γW55 and the α-subunit aromatics estimated by mutant cycle analyses (*SI Appendix*, Fig. S4). pred, predicted $\Delta\Delta G_{B1}$ for the mutant pair (sum of two $\Delta\Delta G_{B1}$ values for single-site mutations); obs, the observed $\Delta\Delta G_{B1}$ for the mutant pair; obs-pred, the coupling energy. γW55A is energetically coupled only to αY93A and αY190A. (*C*) Contribution of functional groups to ΔG_{B1}^{ACh}. The area of each slice is approximately proportional to the free energy lost on removal of each functional group. At αε and αγ, the aromatic groups of αW149, αY190, and αY198 and the hydroxyl of αY190 make approximately equal contributions. At αγ, W55 makes a huge contribution (~−4.5 kcal/mol), and the aromatic group of αY93 contributes about as much as αY198. Thick line, loop C contribution.

we get $\Delta G_{B1} \sim G_{LA}$. Hence, in this regard, the energy difference from the affinity change can be compared with the bound vs. unbound energy difference. A second issue is that energies from simulations are enthalpies (ΔH_{B1}) that do not incorporate entropy (ΔS_{B1}), whereas ΔG_{B1} measurements from electrophysiology are free energies that report both enthalpy and entropy contributions ($\Delta G_{B1} = \Delta H_{B1} - T\Delta S_{B1}$, where T is the absolute temperature). Previously, energy measurements as a function of temperature showed that relative to ACh, the change in (ΔG_{B1}+ ΔG_{B2}) was approximately equal to the change in ($\Delta H_{B1} + \Delta H_{B2}$) for both CCh and Cho (23). This suggests that the entropy component of the agonist's free energy change is small and, hence, that it is appropriate to compare free energies from experiments with enthalpies from simulations.

Fig. 5*A* shows the distributions of simulated ΔG_{B1}^{ACh} values for each site. As with the electrophysiology ΔG_{B1}^{ACh} values, the population means were in the order αγ>αδ~αε. Moreover, experiments and simulations produced results that were in good quantitative agreement, with both indicating ~33% more energy from αγ relative to αδ/αε (Fig. 5*B* and *SI Appendix, Methods*). A breakdown of the simulated enthalpy at each site into its various components is shown in *SI Appendix*, Fig. S5. The three binding sites were broadly similar in their dynamics, as evidenced by the similar root-mean-square fluctuations profiles (*SI Appendix*, Fig. S6). As expected, loop regions in both sides of the binding pocket were more flexible at all three sites. The most flexible regions on the α-side were loops C and F, which were less dynamic in αγ compared with αδ and αε.

Fig. 5*E* shows representative snapshots of the two fetal-type AChR agonist sites, αγ and αδ, obtained from MD simulations of heteropentamers. Simulations of αε, αδ, and αγ dimers produced similar results (*SI Appendix*, Fig. S7 and Table S8). At αγ, the five aromatic side chains make up a tight pocket that is ~22% smaller than at αδ (Fig. 5*C*) and is similar to the starting acetylcholine binding protein structure (11). In contrast, in the course of the simulations, the W55, αY93, and αW149 side chains at the αδ and αε sites separate from ACh quaternary ammonium (QA), and the angle between the two indole planes becomes less orthogonal.

Discussion

Free Energy Measurements from Electrophysiology. The agonist sites of muscle AChRs operate approximately independently, insofar as the sums of the one-site ΔG_{B1}^{ACh} values are approximately equal to those from site pairs (Fig. 2*D*). In this regard, it is noteworthy that αδ provides about the same agonist-binding free energy, regardless of whether the companion agonist site is αε or αγ. The ~250 amino acid substitutions between the ε and γ subunits apparently have little effect on the resultant αδ agonist free energy. Further, alanine mutations of the aromatic residues at each site have approximately independent energetic consequences and, hence, do not create a newfound interdependence. These results, and others reported elsewhere (24), are consistent with the idea that ΔG_{B1} is generated mainly by local interactions between the agonist and a few structural elements at each binding site. With regard to binding free energy, each agonist site can be considered a small and independent working part of the larger AChR complex. We did, however, find some evidence for intersite ΔG_{B1} coupling for αW149A, where the loss in ACh free energy from the mutant pair was ~0.5 kcal smaller than for αδ+αγ sum.

The above observations regarding site independence pertain only to ΔG_{B1} and do not rule out the possibility that the sites are coupled energetically in other ways. For example, mutations of two prolines in the nonα sides of the binding pockets (that do not influence ΔG_{B1}) interact energetically in unliganded gating by ~+0.7 kcal/mol (20). Coupling energies of ~±0.5 kcal/mol are common throughout the AChR (24), so there may be a general, low-level transfer of free energy over distance, side chain to side chain (most mutations do not probe the backbone). Such energy transfer may be important in the gating isomerization, even if it does not substantially influence ΔG_{B1}.

The three kinds of AChR agonist site are not equivalent. The agonist affinity change generates ~−2 kcal/mol more favorable free energy at the fetal, αγ, site than at αδ for all four tested ligands. The adult, αε, site is, in general, similar to αδ but shows an even less favorable free energy change for Cho. At αε and αδ, only three aromatic groups (the indole of αW149 and the benzenes of αY190 and αY198) contribute significantly to ΔG_{B1}^{ACh}, each by ~−2 kcal/mol each. At αγ, however, all five aromatic groups participate. Here, the rings of αW149, αY93, and in particular, γW55 provide free energies that are ~−0.8, −1.7, and −4.5 kcal/mol more favorable for ACh than at αδ, respectively (Fig. 4*E*). The sum of the extra energies from these three residues is more than enough to account for the total extra free energy at αγ.

By far the largest difference in experiments between αγ and αδ/αε was with regard to W55. The deletion of this tryptophan

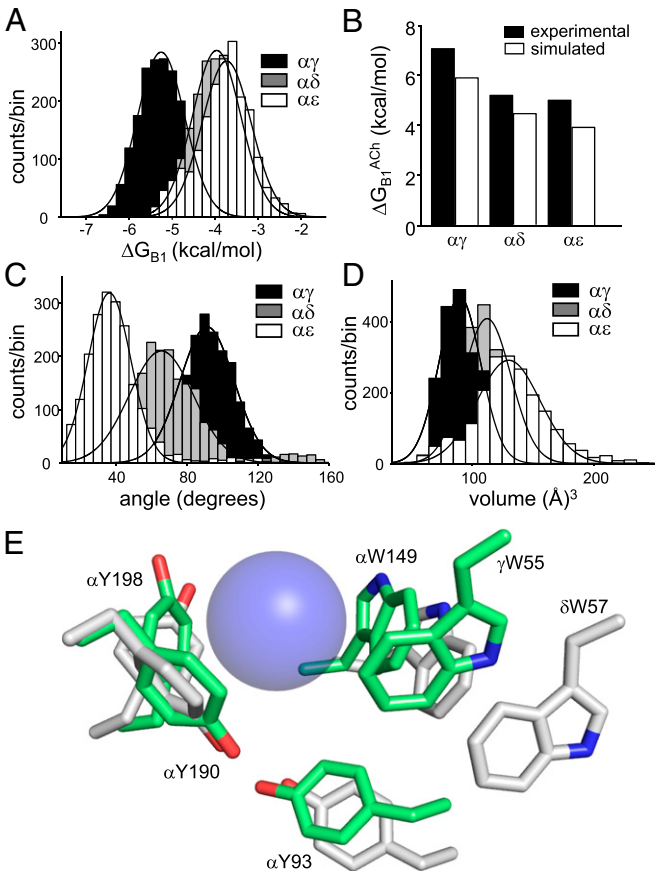

Fig. 5. Simulated ACh binding energies and structural parameters. (*A*) ΔG_{B1}^{ACh}. The mean energy is ~33% more favorable at αγ compared with αδ and αε (*SI Appendix*, Table S6). (*B*) Experimental (black) vs. simulated (white) ΔG_{B1}^{ACh} at each site (αγ>αδ~αε). (*C*) Angle between the W55 and αW149 indole rings. The planes are orthogonal only at αγ (*SI Appendix*, Table S7). (*D*) Volume of the agonist binding pocket. αγ is the most compact (*SI Appendix*, Table S8). (*E*) Representative snapshots of αγ and αδ (pentamer simulations). Blue sphere, QA of ACh (approximately as a van der Waals surface). At αγ (green), W55, αY93, and αW149 are closer to the QA compared with at αδ (white). These three amino acids also show the largest differences in experimental ΔG_{B1}^{ACh} between sites (−1.7, −0.8, and −4.5 kcal/mol, respectively). The orientations of αY198 and αY190 relative to the QA are similar at both sites, as are the effects of mutations of these residues on ΔG_{B1}^{ACh} (*SI Appendix*, Table S4). A representative snapshot of αε is shown in *SI Appendix*, Fig. S7.

had no effect in αδ and only a modest one at αε, but resulted in a huge loss of favorable binding energy at αγ (more than for any other single residue). The reduction in agonist energy at αγ consequent to the γW55A substitution is massive. In fetal AChRs, >35% of the total energy for gating from two neurotransmitter molecules is lost with the γW55A mutation. The W55 side chain in the nonα subunit is an important and variable source of energy at nicotinic AChR binding sites (a "variac").

Although αY190 behaves similarly at all three binding sites, this residue deserves special mention because the effects of an A substitution here are so large (nearly +4 kcal/mol per site). This energy is split approximately evenly between the –OH group and the aromatic ring at all three types of site. In contrast, the –OH groups of αY198 and αY93, which have similar behaviors at all three sites, make much smaller contributions to ΔG_{B1}^{ACh} (Fig. 4*A*). Experiments indicate that the αY190 hydroxyl makes a hydrogen bond with αK145 (25), and simulations suggest an interaction of this group with αY93 (26).

We can think of three possibilities for the large energetic effect of the αY190F mutation: this –OH group interacts directly and favorably with the agonist's QA; the interaction between the αY190 aromatic ring and the QA (likely cation-π) is approximately twice as large with vs. without this H bond (−3.8 vs. −1.9 kcal/mol) because of a difference in the ring's local orientation, electronic character (27), or both; or the αY190 H-bond acts indirectly to shape the overall binding pocket and allow other aromatic groups to interact more favorably with the QA. The marked difference between the αY190F and αY198F/αY93F mutations suggests that the first possibility is unlikely, and the small interaction free energies between αY190F-αW149F [in adult AChRs (18)] and αY190F-γW55A (Fig. 4*C*) suggest that the deletion of the αY190 H-bond does not result in a general reorganization of the binding pocket. We therefore favor the hypothesis that the αY190 hydroxyl group serves to strengthen local, favorable interactions between its aromatic ring and the QA, but more experiments are needed.

The electrophysiology results suggest that the ΔG_{B1}^{ACh} contributions of loop C residues αY190 and αY198 are determined mainly by the α subunit itself, although there is some coupling between αY190F and γW55A. In contrast, the aromatic groups of loop A residue αY93 and loop B residue αW149 make different contributions to ΔG_{B1}^{ACh}, depending on the complimentary, nonα subunit. For example, at αγ, the free energy from the αY93 benzene is more favorable (by ~−1.2 kcal/mol) than at αδ. αY93 and αW149 also showed significant coupling with γW55. It is possible that the nonα subunit has a greater influence on loops A and B and that loop C is a more autonomous structural element of the agonist site.

Simulations. The MD results were broadly consistent with those obtained by electrophysiology. The relative energy differences for ACh at αγ, αε, and αδ were similar (Figs. 5*A* vs. 2*C*; *SI Appendix*, Table S6). Simulations of dimers vs. pentamers produced similar energies and structural parameters, as predicted by the electrophysiology results showing site independence. The model side chain orientations and experimental free energies were also congruent. At all three sites, αY190 and αY198 adopted similar configurations relative to the QA in the simulations and also showed similar experimental free energy values. Likewise, W55, αY93, and αW149 showed the largest structural differences as well as the most free energy variation between sites. The general correspondence between simulations and electrophysiology suggests that the representative snapshots from the simulations (Fig. 5*E*) can be used as a provisional basis for interpreting the experimental ΔG_{B1}^{ACh} differences between the agonist sites. Further examination of the correspondence between simulation predictions and experimental results should reveal the value and limitations of the simple model used in this study.

The forces that undergird the free energy (structure) differences between the three agonist sites are not known. The fact that ACh and tetramethylammonium provide about the same amount of extra free energy at αγ suggests that an interaction of the "tail" of the agonist with the nonα subunit is probably not the reason for the larger energy contributions from W55, αY93, and αW149. Further, the homology models used in the MD simulations were from the same ACh binding protein crystal structure, so neither the overall alignment between the α and nonα subunits nor differences between the backbones of the nonα subunits are likely reasons for the differences between αγ and αδ/αε. By elimination, we postulate that side chains in the ε/δ subunit, which have yet to be identified but probably are in the vicinity of the pocket, make ΔG_{B1}^{ACh} less favorable at αδ/αε compared with αγ. From our experiments, we cannot distinguish whether forces from these side chains generate a stable binding pocket that preexists the arrival of the agonist or whether the arrival of the ligand is an organizing principle that rearranges the αε/αδ site into a suboptimal configuration.

Synapse Development and Physiology. The special character of γW55 has consequences for the cell response. First, the more favorable ΔG_{B1}^{ACh} at αγ enables fetal AChRs to respond to lower

concentrations of the neurotransmitter by virtue of both a higher resting affinity (lower K_d) and a higher efficacy (larger diliganded gating equilibrium constant). From the relationship $\Delta G_{B1} = +0.59\ln K_d$ (*SI Appendix, Methods*), we estimate that at αγ, αε, and αδ K_d^{ACh} = 5, 175, and 200 μM, respectively. Simulations of synaptic responses show that fetal AChRs produce a substantially larger response to the neurotransmitter in the concentration range 10–100 μM (19). Second, the more favorable ΔG_{B1} for choline at αγ enables fetal AChRs to respond to lower concentrations of this physiological ligand. Indeed, ΔG_{B1}^{Cho} at αγ is as favorable as ΔG_{B1}^{ACh} at αε (Fig. 2*C*). Using the above relationship, we estimate that the resting affinities for Cho at αγ, αε, and αδ are K_d^{Cho} = 0.5, 12, and 2.2 mM, respectively. Hence, fetal-type AChRs should produce substantially larger responses to Cho compared with adult-type in the 0.1–1-mM range. This higher sensitivity to Cho could have a synergistic effect on the synaptic current (when approximately millimolar [Cho] may exist, transiently) and lead to increased constitutive activity generated by stable, background Cho in fetal serum (3). There is evidence that the [ACh] is lower at immature vs. mature synapses (28), but it is not known whether fetal AChRs are activated by ambient levels of choline (and to what effect) or, indeed, whether choline is released from the nerve terminal at developing synapses. More experiments are needed to test the hypothesis that the higher sensitivity of fetal AChRs to Cho is a reason that the γ subunit is required for proper maturation of the neuromuscular junction.

One aspect of cation-π forces is that they only derive from protein–ligand interactions and, unlike H-bonds, are newfound energies that are not traded off with those from the solvent. Given the all-or-none nature of the vertebrate neuromuscular synapse, it is curious that neither of the two adult sites (αδ and αε) derive the maximum free energy from the neurotransmitter molecule. It seems that through natural selection, the fetal αγ site has been so optimized, but as a consequence, it responds to Cho as well as ACh. Perhaps the ε subunit, which is evolutionarily more recent than γ (29, 30), has been selected specifically because it does not respond to Cho. We speculate that the differential sensitivity to Cho, which is higher at αγ and lower at αε, is a reason for the γ→ε subunit swap that is required for synapse development (3, 31). Fetal and adult AChRs also differ in conductance, open-channel lifetime, voltage sensitivity, frequency of spontaneous openings, and Ca^{2+} permeability (32). Which of these differences in function are necessary for healthy nerve–muscle synapse development and function remains to be determined.

Methods

Electrophysiological recordings were performed on transiently transfected HEK cells using cell-attached patch-clamp and were analyzed using QUB software (33). The QuikChange site-directed mutagenesis kit was used to mutate AChR subunit cDNAs. Single-channel dwell times were measured to estimate the gating equilibrium constants and free energies. The WT agonist free energies were compared with the energy values calculated from MD simulations. A detailed description of the methods is given in *SI Appendix, Methods*.

ACKNOWLEDGMENTS. We thank M. Merritt, M. Shero, and M. Teeling for technical assistance and the Center for Computational Research, University at Buffalo, for computational facilities. This work was funded by National Institutes of Health Grants NS064969 and NS023513.

1. Monod J, Wyman J, Changeux JP (1965) On the Nature of Allosteric Transitions: A Plausible Model. *J Mol Biol* 12:88–118.
2. Karlin A (1967) On the application of "a plausible model" of allosteric proteins to the receptor for acetylcholine. *J Theor Biol* 16(2):306–320.
3. Zeisel SH, Niculescu MD (2006) Perinatal choline influences brain structure and function. *Nutr Rev* 64(4):197–203.
4. Unwin N (2013) Nicotinic acetylcholine receptor and the structural basis of neuromuscular transmission: Insights from Torpedo postsynaptic membranes. *Q Rev Biophys* 46(4):283–322.
5. Jaramillo F, Vicini S, Schuetze SM (1988) Embryonic acetylcholine receptors guarantee spontaneous contractions in rat developing muscle. *Nature* 335(6185):66–68.
6. Takahashi M, et al. (2002) Spontaneous muscle action potentials fail to develop without fetal-type acetylcholine receptors. *EMBO Rep* 3(7):674–681.
7. Witzemann V, et al. (1996) Acetylcholine receptor epsilon-subunit deletion causes muscle weakness and atrophy in juvenile and adult mice. *Proc Natl Acad Sci USA* 93(23):13286–13291.
8. Auerbach A (2013) The energy and work of a ligand-gated ion channel. *J Mol Biol* 425(9):1461–1475.
9. Cohen JB, Sharp SD, Liu WS (1991) Structure of the agonist-binding site of the nicotinic acetylcholine receptor. [3H]acetylcholine mustard identifies residues in the cation-binding subsite. *J Biol Chem* 266(34):23354–23364.
10. Kearney PC, et al. (1996) Dose-response relations for unnatural amino acids at the agonist binding site of the nicotinic acetylcholine receptor: Tests with novel side chains and with several agonists. *Mol Pharmacol* 50(5):1401–1412.
11. Brejc K, et al. (2001) Crystal structure of an ACh-binding protein reveals the ligand-binding domain of nicotinic receptors. *Nature* 411(6835):269–276.
12. Li L, et al. (2001) The tethered agonist approach to mapping ion channel proteins—toward a structural model for the agonist binding site of the nicotinic acetylcholine receptor. *Chem Biol* 8(1):47–58.
13. Zhong W, et al. (1998) From ab initio quantum mechanics to molecular neurobiology: A cation-pi binding site in the nicotinic receptor. *Proc Natl Acad Sci USA* 95(21):12088–12093.
14. Chiara DC, Cohen JB (1997) Identification of amino acids contributing to high and low affinity d-tubocurarine sites in the Torpedo nicotinic acetylcholine receptor. *J Biol Chem* 272(52):32940–32950.
15. Xie Y, Cohen JB (2001) Contributions of Torpedo nicotinic acetylcholine receptor gamma Trp-55 and delta Trp-57 to agonist and competitive antagonist function. *J Biol Chem* 276(4):2417–2426.
16. Bafna PA, Jha A, Auerbach A (2009) Aromatic Residues epsilonTrp-55 and deltaTrp-57 and the Activation of Acetylcholine Receptor Channels. *J Biol Chem* 284(13):8582–8588.
17. Nowak MW, et al. (1995) Nicotinic receptor binding site probed with unnatural amino acid incorporation in intact cells. *Science* 268(5209):439–442.
18. Purohit P, Bruhova I, Auerbach A (2012) Sources of energy for gating by neurotransmitters in acetylcholine receptor channels. *Proc Natl Acad Sci USA* 109(24):9384–9389.
19. Nayak TK, Auerbach A (2013) Asymmetric transmitter binding sites of fetal muscle acetylcholine receptors shape their synaptic response. *Proc Natl Acad Sci USA* 110(33):13654–13659.
20. Gupta S, Purohit P, Auerbach A (2013) Function of interfacial prolines at the transmitter-binding sites of the neuromuscular acetylcholine receptor. *J Biol Chem* 288(18):12667–12679.
21. Jadey SV, Purohit P, Bruhova I, Gregg TM, Auerbach A (2011) Design and control of acetylcholine receptor conformational change. *Proc Natl Acad Sci USA* 108(11):4328–4333.
22. Purohit P, Bruhova I, Gupta S, Auerbach A (2014) Catch-and-hold activation of muscle acetylcholine receptors having transmitter binding site mutations. *Biophys J* 107(1):88–99.
23. Gupta S, Auerbach A (2011) Temperature dependence of acetylcholine receptor channels activated by different agonists. *Biophys J* 100(4):895–903.
24. Purohit P, Gupta S, Jadey S, Auerbach A (2013) Functional anatomy of an allosteric protein. *Nat Commun* 4:2984.
25. Mukhtasimova N, Free C, Sine SM (2005) Initial coupling of binding to gating mediated by conserved residues in the muscle nicotinic receptor. *J Gen Physiol* 126(1):23–39.
26. Mallipeddi PL, Pedersen SE, Briggs JM (2013) Interactions of acetylcholine binding site residues contributing to nicotinic acetylcholine receptor gating: Role of residues Y93, Y190, K145 and D200. *J Mol Graph Model* 44:145–154.
27. Mecozzi S, West AP, Jr, Dougherty DA (1996) Cation-pi interactions in aromatics of biological and medicinal interest: Electrostatic potential surfaces as a useful qualitative guide. *Proc Natl Acad Sci USA* 93(20):10566–10571.
28. Polak RL, Sellin LC, Thesleff S (1981) Acetylcholine content and release in denervated or botulinum poisoned rat skeletal muscle. *J Physiol* 319:253–259.
29. Ortells MO, Lunt GG (1995) Evolutionary history of the ligand-gated ion-channel superfamily of receptors. *Trends Neurosci* 18(3):121–127.
30. Tsunoyama K, Gojobori T (1998) Evolution of nicotinic acetylcholine receptor subunits. *Mol Biol Evol* 15(5):518–527.
31. Zeisel SH (2006) Choline: Critical role during fetal development and dietary requirements in adults. *Annu Rev Nutr* 26:229–250.
32. Mishina M, et al. (1986) Molecular distinction between fetal and adult forms of muscle acetylcholine receptor. *Nature* 321(6068):406–411.
33. Nicolai C, Sachs F (2013) Solving ion channel kinetics with the QuB software. *Biophysical Reviews and Letters* 08(03):1–21.
34. Unwin N (2005) Refined structure of the nicotinic acetylcholine receptor at 4A resolution. *J Mol Biol* 346(4):967–989.